Fermi National Accelerator Laboratory

FERMILAB-Pub-93/160
(UMAHEP-388, Nevis R1493)

High Rate Drift Chambers

D.C. Christian, M.C. Berisso, G. Gutierrez, S.D. Holmes, A. Wehmann

Fermi National Accelerator Laboratory
P.O. Box 500, Batavia, Illinois 60510

C. Avilez, J. Felix, G. Moreno, M. Romero, M. Sosa

Instituto de Fisica, Universidad de Guanajuato
Leon, Guanajuato, Mexico

M. Forbush, F.R. Huson, J.A. Wightman

Department of Physics, Texas A&M University,
College Station, Texas 77843

A. Gara, B.C. Knapp, W. Sippach

Columbia University, Nevis Laboratories
Irvington, New York 10533

E.P. Hartouni, D.A. Jensen, M.N. Kreisler, S. Lee, K. Markianos, D. Wesson

Department of Physics and Astronomy, University of Massachusetts
Amherst, MA 01003

June 1993

Submitted to *Nuclear Instruments & Methods in Physics Research*

Disclaimer

Fermi National Accelerator Laboratory

FERMILAB-Pub-93/160
(UMAHEP-388, Nevis R1493)

HIGH RATE DRIFT CHAMBERS

D.C. CHRISTIAN, M.C. BERISSO[1], G. GUTIERREZ, S.D. HOLMES,
A. WEHMANN
Fermilab, Batavia, IL 60510

C. AVILEZ[2], J. FELIX, G. MORENO, M. ROMERO, M. SOSA
Instituto de Física, Universidad de Guanajuato, Léon, Guanajuato, México

M. FORBUSH[3], F.R. HUSON, J.A. WIGHTMAN
Department of Physics, Texas A&M University, College Station, TX 77843

A. GARA, B.C. KNAPP, W. SIPPACH
Columbia University, Nevis Laboratories, Irvington, N.Y. 10533

E.P. HARTOUNI, D.A. JENSEN[4], M.N. KREISLER, S. LEE, K. MARKIANOS,
D. WESSON
Department of Physics and Astronomy, University of Massachusetts,
Amherst, MA 01003

[1] Present address: University of Massachusetts, Amherst, MA 01003
[2] Deceased
[3] Present address: University of California, Davis, CA 95616
[4] Present address: Fermilab, Batavia, Il 60510

June 1993

* Submitted to *Nuclear Instruments & Methods in Physics Research*

HIGH RATE DRIFT CHAMBERS

D.C. CHRISTIAN, M.C. BERISSO[1], G. GUTIERREZ, S.D. HOLMES,
A. WEHMANN
Fermilab, Batavia, IL 60510

C. AVILEZ[2], J. FELIX, G. MORENO, M. ROMERO, M. SOSA
Instituto de Física, Universidad de Guanajuato, Léon, Guanajuato, México

M. FORBUSH[3], F.R. HUSON, J.A. WIGHTMAN
Department of Physics, Texas A&M University, College Station, TX 77843

A. GARA, B.C. KNAPP, W. SIPPACH
Columbia University, Nevis Laboratories, Irvington, N.Y. 10533

E.P. HARTOUNI, D.A. JENSEN[4], M.N. KREISLER, S. LEE, K. MARKIANOS,
D. WESSON
Department of Physics and Astronomy, University of Massachusetts,
Amherst, MA 01003

[1] Present address: University of Massachusetts, Amherst, MA 01003
[2] Deceased
[3] Present address: University of California, Davis, CA 95616
[4] Present address: Fermilab, Batavia, Il 60510

Abstract

Fermilab experiment 690, a study of target dissociation reactions $pp \rightarrow pX$ using an 800 GeV/c proton beam and a liquid hydrogen target, collected data in late 1991. The incident beam and 600-800 GeV/c scattered protons were measured using a system of six $6" \times 4"$ and two $15" \times 8"$ pressurized drift chambers spaced over 260 meters. These chambers provided precise measurements at rates above 10 MHz (2 MHz per centimeter of sense wire). The measurement resolution of the smaller chambers was 90 μm, and the resolution of the larger chambers was 125 μm. Construction details and performance results, including radiation damage, are presented.

Introduction

The FNAL E690 apparatus consisted of a high rate, open geometry multiparticle spectrometer used to measure the target system (X) in $pp \rightarrow pX$ reactions, and a beam spectrometer system used to measure the incident beam and scattered proton. In a data-taking period of 100 days, 5.4×10^9 events were written to tape. The initial goals of the analysis of these data include the study of heavy flavor production (strange and charm) in the target fragmentation region and the study of light meson

production in the central region. Much of the analysis will concentrate on all charged exclusive final states in which energy and momentum constraints facilitate the unambiguous identification of every final state particle. In order to isolate a large sample of exclusive reactions, the spectrometer, especially the beam system, was designed to have very good momentum resolution and very high rate capability. To achieve these goals, the beam spectrometers used very long lever arms, large bends, and a system of small cell, pressurized drift chambers (minidrift PWC's). In this paper construction details, performance results, and the effects of radiation damage on these beam chambers are presented.

Construction Details/Specifications

Two types of chambers were used in the E690 beam spectrometers. Each type consisted of four sense planes, five shared cathodes, and two ground planes (see Fig. 1). Mechanical rigidity was provided by aluminum clamping frames. All of the anodes and cathodes were supported on frames milled from 1/16" thick FR-4 fiberglass sheet material and ground to a uniform thickness of 55 mils. A 32 mil step surrounding the active area was machined into each frame on the side opposite the electrode. A sheet of 0.5 mil Kapton with a rectangular hole the size of the active area of the chamber was glued to the frame in this stepped

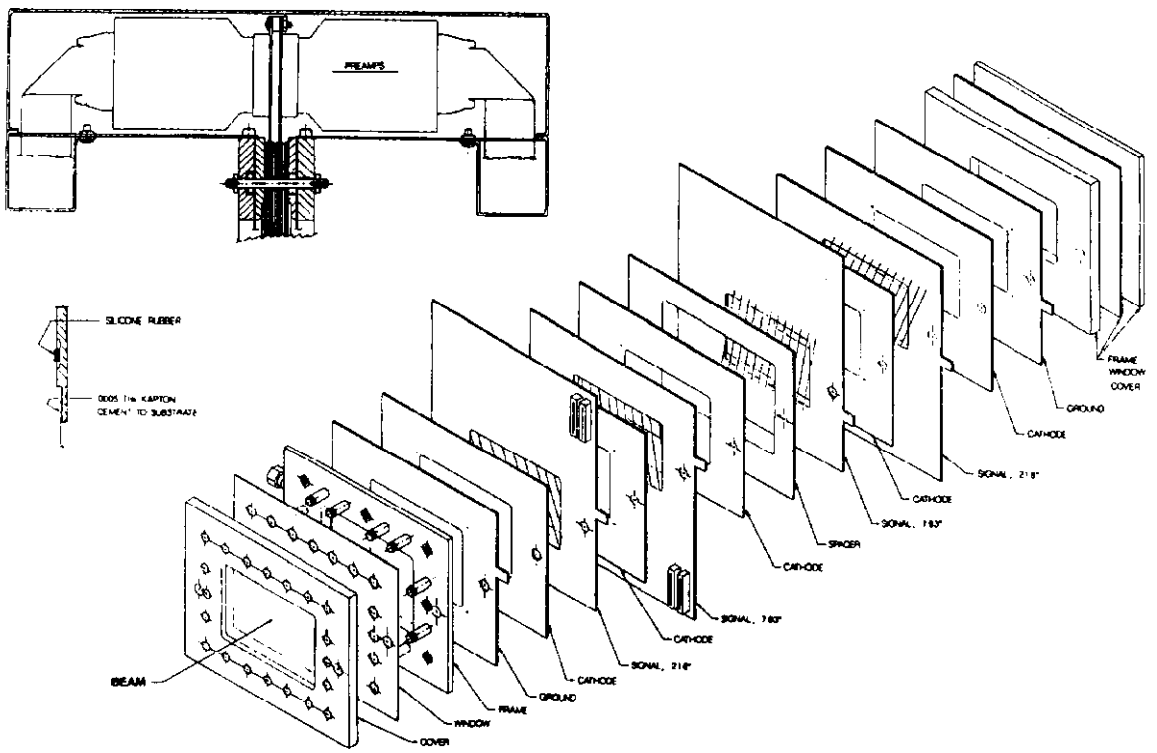

Figure 1: Assembly drawing for 6" × 4" aperture chambers; the assembly details for the 15" × 8" chambers are very similar.

region. The Kapton projected into the gap between anode and cathode and helped prevent electrostatic breakdown at the aperture edge. A 20 mil deep gasket groove was machined into the same side of each frame as the step (see Fig. 1). Gas seals were made with dry gaskets of soft (30 durometer) silicon rubber cut from 1/32" thick sheet material. All of the planes were oriented so that the gasket groove was towards the outside of the stack of planes and the electrode towards the center of the

stack. The gas seal in the middle of the stack was made by a spacer plane which did not carry an electrode and had gasket grooves on both sides.

The signal planes were wound with Tungsten-Rhenium alloy wire (3% Rh), gold plated to 3-5% by weight. Winding was done using a precision winding machine built at Fermilab. The wires were secured by a thin bead of epoxy (less than 15 mils thick), and soldered to copper traces on the FR-4 boards. Both the glue bead and the solder connections were located in the space close to the active region that was covered by the step in the next board in the chamber stack. The four planes in a chamber were oriented at angles of -21.6, -7.93, 7.93, and 21.6 degrees with respect to the shorter axis of the rectangular aperture. Detailed specifications for both types of chamber are listed in Table 1.

The aluminum foil cathodes and ground planes were glued to lucite rings which had been cooled in a household freezer, and stretched by the expanding lucite as it warmed to room temperature. The ground planes were then glued to copper clad FR-4 using conductive epoxy. The cathode foils were glued to their FR-4 frames using a bead of Eastman 910 adhesive. A very thin Teflon insulated wire was glued using conductive epoxy to the edge of the cathode foil and extended to the outside of the frame in a shallow groove in the FR-4 frame. To protect against high voltage leakage current, the insulation was stripped from this wire only inside the gas seal. After the wire was in place, the groove in the FR-4

SPECIFICATIONS

	Smaller Chambers		Larger Chambers	
Horizontal Aperture	6	inches	15	inches
Vertical Aperture	4	inches	8	inches
Anode Wire Spacing	0.040	inches	0.060	inches
Anode Wire Diameter	12	microns	15	microns
Anode Wire Tension	20	grams	35	grams
# of Wires / Plane	160		256	
Plane-Plane Gap	0.055	inches	0.055	inches
Cathodes	0.5	mil hard temper Al. foil	0.5	mil hard temper Al. foil
Ground Planes	0.5	mil hard temper Al. foil	1	mil hard temper Al. foil
Windows	2	mil Kapton + 1.7 oz/yd^2 Kevlar cloth (Operation @ 30 psig)	10	mil Mylar (Operation @ 7 psig)
Material in Radiation Lengths	0.24	%	0.39	%
Material in Interaction Lengths	0.06	%	0.12	%

Table 1

was filled with glue and sanded smooth so that it would not cause a gas leak. The five cathodes were connected through current limiting resistors (typically 1 MΩ) to a common high voltage connector.

All of the chambers were operated with a gas mixture consisting of 82% Argon, 15% Isobutane, and 3% Methylal. The smaller chambers were operated at pressures up to 30 psig. This pressure was contained by windows consisting of a sheet of 2 mil Kapton clamped to a layer of 1.7 oz/yd^2 Kevlar cloth. The Kevlar cloth [*] was oriented with the bias along the short vertical span (so that all fibers were at 45° with respect to vertical). This allowed the cloth to deform and spread the load evenly. The choice of orientation of the weave was a result of tests to determine the pressure at which the windows failed. These tests were performed using two window clamping frames placed back to back with only a water volume in between. The water pressure was increased until one window failed. In tests with the Kevlar oriented with fibers in the direction of the short span, the fabric did not stretch to distribute the load evenly. Instead, a small number of fibers took the entire load and broke at fairly low applied pressure. This caused the fabric to develop a "run" after which the Kapton window quickly ruptured. With the fibers at 45° with respect to the short span, a test window failed at 75 psig.

---

* Purchased from Hi-Pro-Form-Fabrics, Inc. Newark, Del. Designated as "style 120"; plain weave Kevlar 49, 1.7 oz/yd^2. Through holes for the bolts used to clamp the window frames together were drilled in the cloth using a bit made by sharpening a punch. This cloth represents 1.35×10^{-4} radiation lengths of material, which is less than the 2 mils of Kapton used as a gas seal.

The larger chambers were not operated above 7 psig. At higher pressure, the frames distorted slightly and released the tension in the outer aluminum foil planes enough to allow breakdown between the outer cathodes and the ground planes.

Use of "PWC" Geometry for Drift Chambers

Drift chambers are usually built with field shaping electrodes in addition to anodes and cathodes. For chambers with long drift distances, this is necessary to assure a large uniform drift velocity. One might assume that small and moderately sized drift chambers designed with short drift distances for high rate capability also require field wires in the anode plane to avoid problems in the region of zero field. The success of our simple "pwc" design demonstrates that there is no limitation caused by electrons slowly diffusing out of a dead region. In fact, field wires in the anode plane are not only unnecessary and very difficult to provide, but they also reduce measurement resolution.

Consider the details of the signal detection and the measurement of the drift time. Electrons ionized along the trajectory of the high energy particle drift along field lines to the nearest anode. These electrons have the statistical fluctuations of the production of primary ionization and subsequent diffusion. The average drift time for electrons on a particle

trajectory has a minimum, usually at the point closest to the anode. For tracks with a fixed angle of incidence, this minimum drift time is a monotonically increasing function of the distance of closest approach of the trajectory to the anode wire. As the minimum drift time increases, so does the length of the trajectory with the same minimum drift time, effectively improving the rise time of the signal at the anode. If the trajectory passes very close to the anode, the number of electrons arriving at the beginning of the pulse is small, resulting in a signal with a poorly defined leading edge. A track with normal incidence to the anode plane, passing halfway between anode wires, has a well-defined shortest drift time, with a large number of electrons arriving together at the longest drift time. If there were a field wire between anode wires, this focusing effect would be lost. The number of electrons near the minimum drift time would decrease as the trajectory approached the field wire, causing the measurement of drift distance to deteriorate near the field wire.

Performance in E690

Efficiency

All eight chambers were checked for gain uniformity at installation and after all repairs. This test was done using an Fe^{55} source, a "pickoff amplifier" (Fig. 2) and a Tektronix 2440 digital oscilloscope. The

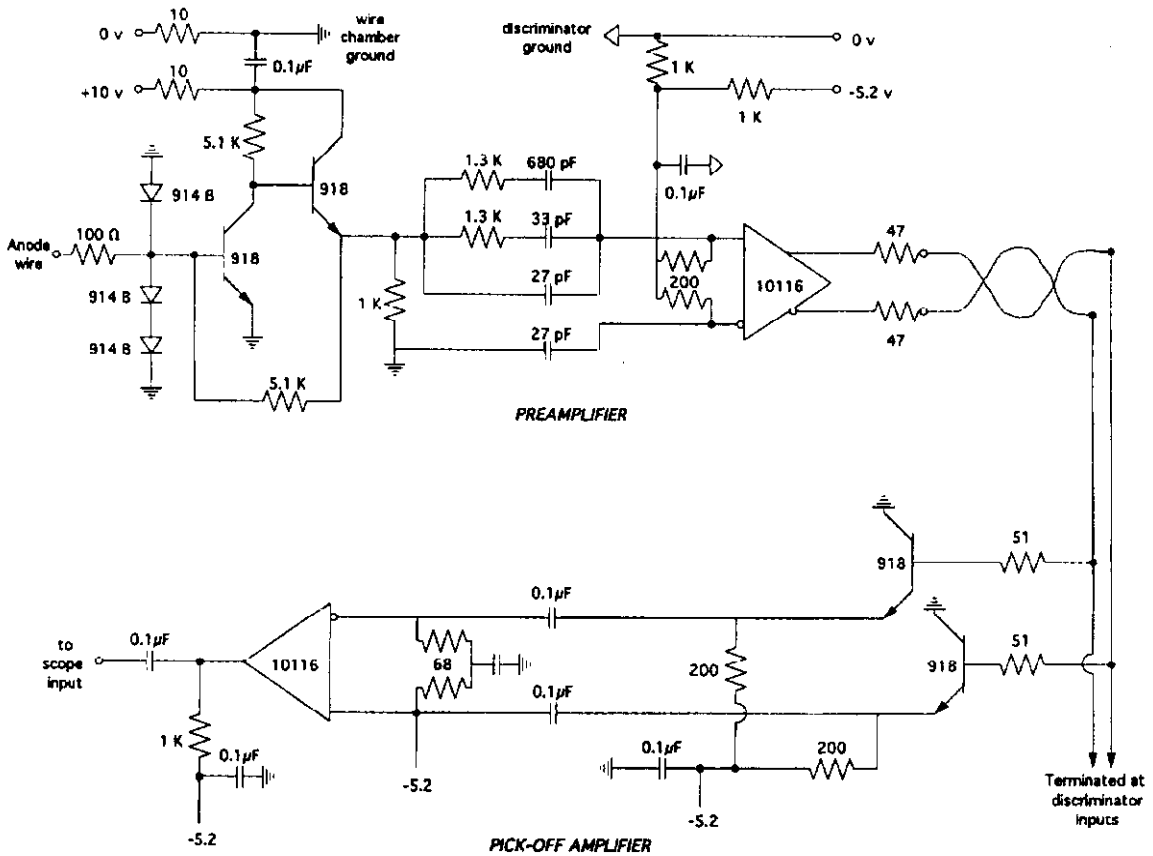

Figure 2: Wire chamber preamplifier and "pick-off" amplifier used with Fe^{55} source and Tektronics 2440 digital oscilloscope for gain measurements.

chamber under test was operated with reduced high voltage to avoid saturation of the preamplifier output. The oscilloscope trigger level was set high enough so that signals from the escape peak did not cause a trigger, and the scope was set to average 256 pulses. This allowed a reproducible measurement of the gain to be made for any given channel.

Gain variations within a plane were typically 10%, which is consistent with expected channel to channel differences in the preamplifiers. Plane-to-plane differences were larger, with the highest gain plane typically 40% higher than the lowest gain plane. Presumably, these differences were the result of variations in the size of the gap between anodes and cathodes, caused by differences in the thickness of the glue beads holding the cathode foils or other similar construction imperfections. The smaller chambers had wide enough voltage plateaus so that all planes could operate efficiently, even with as much as a factor of two gain difference between planes. The larger chambers did not have as large a margin for error, primarily because of the cathode to ground plane breakdown described above. The gain variations in one of the larger chambers were severe enough that it did not operate efficiently above atmospheric pressure without sparking, even after having been rebuilt twice. In order to equalize the gains for this chamber, "9 volt" batteries were added in series with the center cathode (decreasing the voltage by 29.5 volts) and one outer cathode (increasing the voltage by 47 volts). With this modification, the chamber operated at 7 psig with all planes fully efficient.

During data taking, the chambers were operated with a gas gain of approximately 10^5. [*] Preamplifiers mounted on the chambers drove

* This number is based on the current drawn from the high voltage power supplies at known beam rates, and an estimate of the number of primary ionization electrons produced by each beam particle.

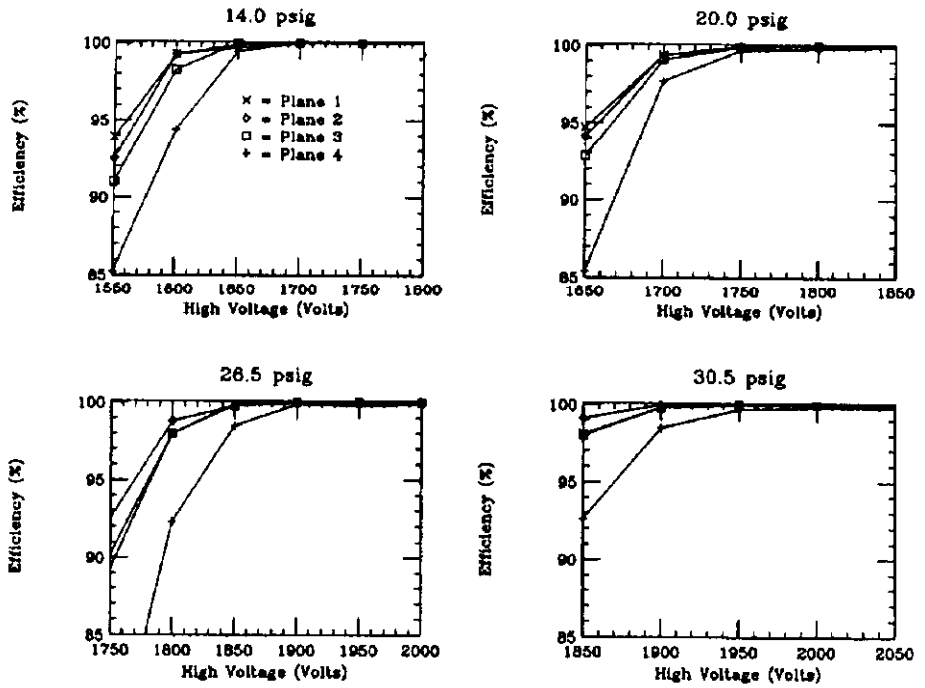

Figure 3: Typical efficiency plateau curves for one of the 6" × 4" aperture chambers.

small differential signals to leading edge discriminators. The discriminators drove differential ECL signals to purely digital TDC's. The TDC's encoded drift time using 2.5 nsec bins. Given an average electron drift velocity in the gas mixture used of approximately 40 μm/nsec, this bin width corresponds to ~100 μm in a chamber.

Typical efficiency plateaus are shown in Fig. 3. [*] As expected, the knee of the curve moves to higher voltage as a linear function of the operating pressure. This figure also illustrates the typical plane-to-plane gain variation within a chamber; in this chamber, plane 4 required higher voltage to achieve full efficiency than the other three planes. In every case, the operating voltage was set at least 50 volts above the knee in the efficiency plateau of the lowest gain plane in a chamber.

The maximum rate at which the chambers could be operated was given by the occupancy and the electronic memory time. The electronic memory time was equal to the spread of leading edge time (15-20 nsec) plus the width of the discriminator pulse (15 nsec). With only eight wires illuminated in the most upstream chamber, we chose not to run above 2.4×10^8 protons per 20 second spill (12 MHz average; 25-30 MHz instantaneous). Most of the E690 data was taken with a beam rate of 1×10^8 per spill. This corresponds to an average rate of 5 MHz, and an instantaneous rate of 10-12 MHz (approximately 2 MHz/cm of sense wire). All planes remained fully efficient ($\gtrsim 99.9\%$) at these rates.

---

* The efficiency of plane n is defined as:

$$\frac{\text{(The number of tracks with no missing measurement)}}{\left(\begin{array}{c}\text{The number of tracks with}\\ \text{no missing measurement}\end{array}\right)+\left(\begin{array}{c}\text{The number of tracks missing}\\ \text{only a measurement from plane } n\end{array}\right)}$$

Measurement Resolution

Scattered high energy protons from data taken in the middle of E690 with a beam rate of approximately 10^8 per spill were used to determine the spatial resolution of the chambers. In order to determine how to map measured drift times into drift distances, a sample of events was chosen in which every plane of every chamber contained either one hit or two adjacent hits. Using these events, a separate time distribution histogram was constructed for each wire of every chamber. When a plane had one hit, the associated drift time was entered with a weight of one. When a plane had two hits, the hit with the larger time was ignored, and the shorter time was entered with a weight of one. If both hits had the same time, both were entered with a weight of 1/2. Time to distance maps were then constructed assuming that these distributions resulted from uniform (or at worst linearly varying) illumination of the drift cells:

$$d(t_i) = \tfrac{1}{2}\,(\text{wire spacing})\,\frac{\left[\sum_{j=t_{\min}}^{i-1} N(t_j)\right] + \tfrac{1}{2}N(t_i)}{\sum_{k=t_{\min}}^{t_{\max}} N(t_k)}$$

($t_{\min}$, $t_{\max}$ = the first and last time bins populated by in-time hits.)

Tracks were found and fit using all but one of the 32 planes of the 8 chambers. The track position in the 32nd plane was calculated and the

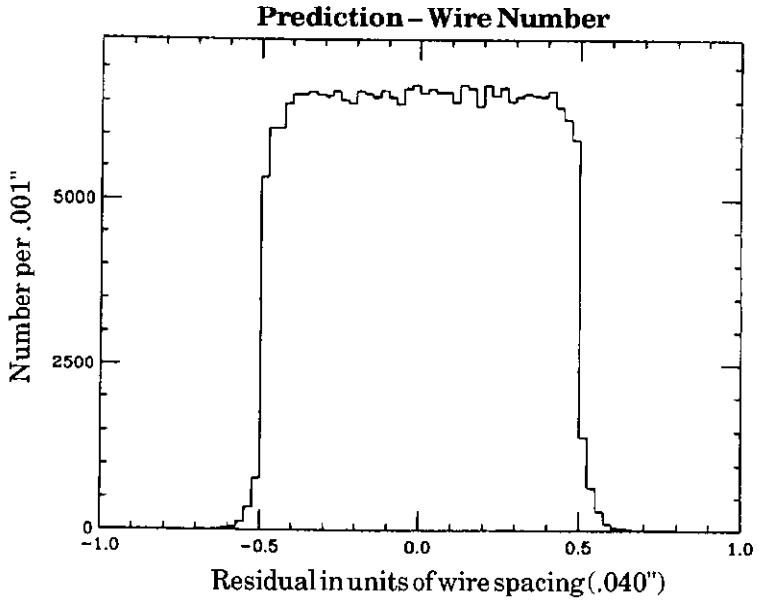

Figure 4: Typical residual distribution for one plane of a smaller chamber (without drift times). The rms of this distribution is .291 (in units of 1 wire spacing = .040"). The inferred prediction error is 35 μm.

difference between this position and the coordinate of the closest hit wire was computed. If the track fits were perfect and the plane under study were 100% efficient, the distribution of (prediction-measured wire number) would be a square with a full width of one wire spacing and an rms of $1/\sqrt{12}$ of a wire spacing. All of the planes were essentially 100% efficient, so once systematic alignment errors are removed, the deviation of this distribution from a square shape can be ascribed to the random error in the prediction of the track coordinate given by the fit. The variance of the prediction can be estimated by subtracting 1/12 of

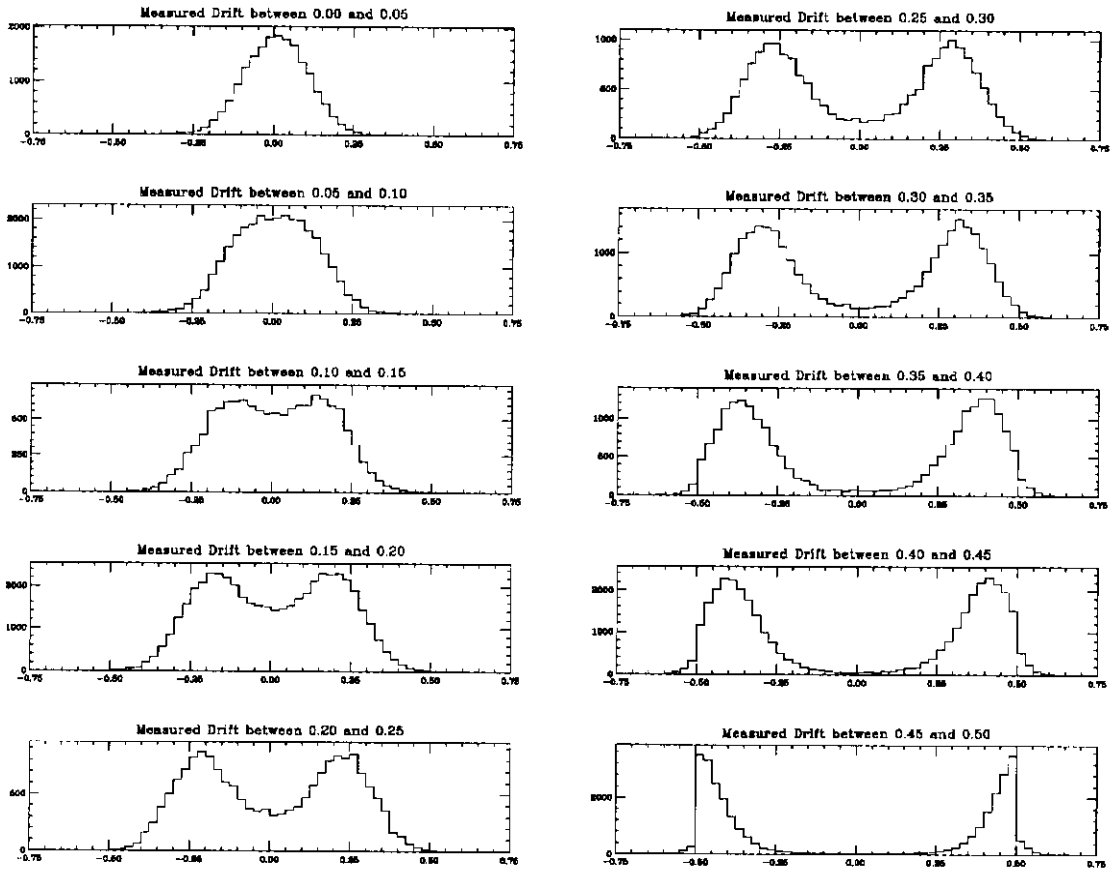

Figure 5: (Prediction-wire number) for slices of the measured drift distance – these distributions are for the same events as in Fig. 4.

a (wire spacing)^2 from the variance of the measured distribution. A typical distribution for one of the smaller chambers is shown in Fig. 4. The rms prediction error inferred from this distribution is 35 μm.

Figure 5 shows the same residual distribution (prediction-measured wire number) as in Fig. 4, as a function of the measured drift

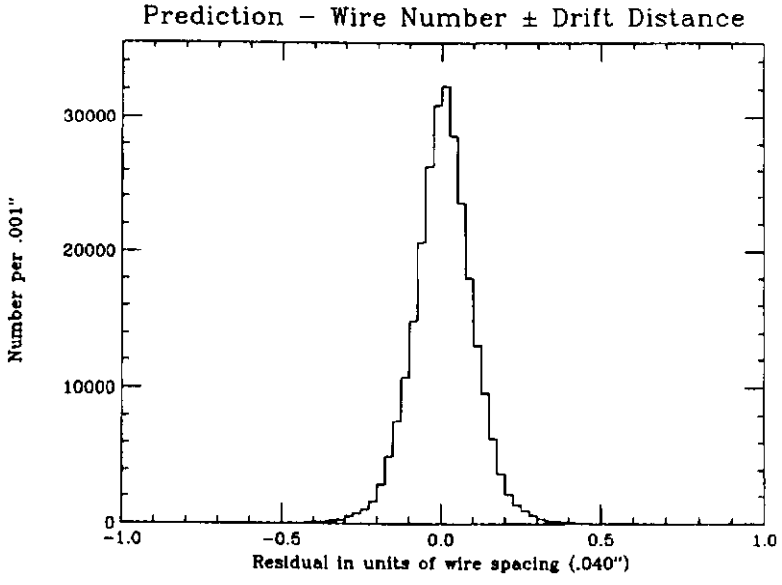

Figure 6: Residual distribution for the same events as in Figures 4 & 5, including drift information. The rms of this distribution is .095 (in units of 1 wire spacing = .040"). The inferred rms measurement error is 90 μm.

distance. This figure demonstrates that the measured drift times are very strongly correlated with the distance of a track from the wire, as expected, and that the left/right assignment can be made unambiguously, except for very short drift times, simply by assigning a sign to the drift measurement based on which side of the wire the prediction is on. The corresponding residual distribution, including drift measurement, is shown in Fig. 6.

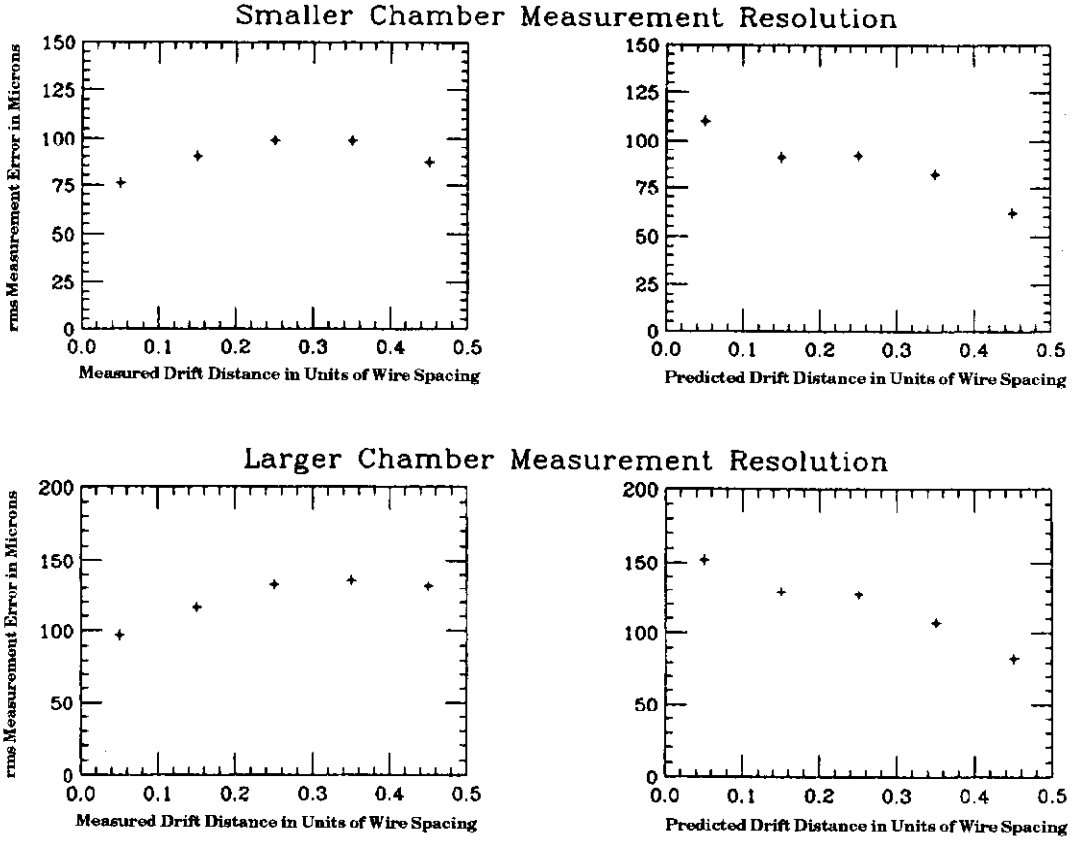

Figure 7: Measurement error as a function of measured drift distance from the closest wire and as a function of predicted distance from the closest wire.

The measurement resolution is calculated by subtracting the rms prediction error in quadrature from the rms of the residual distribution calculated using drift times. For the smaller chambers operating at 30 psig, the rms measurement error was 90 μm. For the larger chambers operating at 7 psig the measurement error was 125 μm.

We have also computed residual distributions separately for bins of measured drift distance. As is shown in Fig. 7, the measurement resolution is not a strong function of the measured drift time. Figures 5 and 7 also illustrate the focusing effect described above; tracks that pass very close to the wire are usually associated with short times, but are occasionally associated with long times and hence are most poorly measured. Tracks that pass near a cell boundary are always associated with long times and are measured best.

Radiation Damage

The current drawn from the high voltage power supplies was used to estimate the amount of charge per unit length of sense wire collected in the beam spot by each chamber. For the small beam chambers, 12 μmA was drawn at an intensity of 8×10^7 protons per 20 second beam spill. In the most upstream beam chamber, the beam spot illuminated 0.6 cm of eight wires approximately uniformly. This implies 1.56×10^{-13} Coulomb/cm of wire was accumulated per beam proton. The area of the beam spot was roughly the same (~0.5 cm^2) in all of the small beam chambers. Since the high voltage current drawn was also roughly the same, the charge accumulated per unit length of signal wire was approximately equal for all of the small chambers.

We have used the computer log of beam flux as measured by an ion chamber located at the end of the forward beam spectrometer (kept by the FNAL Operations Department) to estimate the total beam flux seen by the chambers. The integrated flux recorded by this ion chamber during periods when the beam chambers were at operating voltage was 5.6×10^{12} protons. This means that the average charge accumulated by sense wires in the beam spot was 0.87 C/cm.

The beam spot was small compared to the active area of the three chambers which measured the incident beam. In order to minimize radiation damage effects, these three chambers were moved twice during the run so that no spot accumulated more than an average of 0.36 C/cm of charge. About half way through the run (after an average exposure of 0.43 C/cm), a small decrease in efficiency in the beam spot was noticed for one of the three small beam chambers in the forward spectrometer. The high voltage for all three of these chambers was increased (from 2000 V to 2100 V) for the duration of the run. This restored the affected chamber to full efficiency. The two larger chambers lost efficiency in the beam spot even more quickly. Since these two chambers were operating closer to breakdown, it was not possible to restore full efficiency in the beam spot by increasing their high voltage.

No increase in the amount of current drawn at a given beam rate and high voltage was observed for any of the eight chambers. The TDC

distributions for the small beam chambers which were not moved were broadened for hits in the beam spot. This was not correlated to a dramatic decrease in position resolution.

We have measured the loss of gain in one of the three chambers which measured the incident beam. This measurement was made (one year after the end of the run) using a collimated Fe^{55} source and the setup described above. For wires exposed to an average of 0.36 C/cm, the gain in the beam spot was measured to be approximately a factor of two lower than outside of the beam spot.

Chambers which have been disassembled all have obvious discolored spots in the shape of the beam, both on the anode wires, and on the aluminum foil cathodes. The anodes appear black in the beam spot. No points or hairs are evident. The black material can be washed off (with some difficulty) with ethyl alcohol, isopropyl alcohol, or acetone. The cathode foils have a white deposit in the beam region. Cathode deposits made by shorter beam exposures are in the form of stripes located *between* the signal wires. This is easily understood if one assumes first that the avalanche at the signal wire is localized, rather than encompassing the wire, and second, that the whitish deposit is carried to the cathode by positive ions. The white film is very difficult to wash off. The only solvent which has been at all effective is THF (tera hydro furan).

Conclusions

"Conventional" multiwire proportional chambers, operated as small cell drift chambers, performed very well for an extended run in FNAL E690. No unexpected effect limited the chambers' instantaneous rate capability, even at rates exceeding 2 MHz per centimeter of sense wire. Gain loss, due to radiation damage, was observed after an exposure of $\sim 4.5 \times 10^{12}$ protons/cm^2 (0.36 C/cm), and would have become a problem in a significantly larger exposure. Presumably, the chamber lifetime could be extended by at least a factor of ten by operating at lower gas gain with higher gain preamplifiers.

Acknowledgments

We thank Karen Kephart, Wanda Newby, and Eileen Hahn, of the Fermilab Physics Section, for help with the construction of the chambers described in this paper. Special thanks go to Frank Juravic, also of the Fermilab Physics Section, who not only helped with chamber construction, but also contributed greatly to their design and to the development of successful construction methods.

This work was funded in part by the Department of Energy under contract numbers DE-AC02-76CHO3000 and DE-AS05-87ER40356,

the National Science Foundation under grant numbers PHY89-21320 and PHY90-14879, and CONACyT de México under grant numbers 1061-E2901 and F246-E9207.